Neutralization of IFN defeats haemophagocytosis in LCMV-infected perforin- and Rab27a-deficient mice

Pachlopnik Schmid, Jana ; Ho, Chen-H ; Chrétien, Fabrice ; Lefebvre, Juliette M ; Pivert, Gérard ; Kosco-Vilbois, Marie ; Ferlin, Walter ; Geissmann, Frédéric ; Fischer, Alain ; de Saint Basile, Geneviève

Abstract: Hereditary haemophagocytic lymphohistiocytosis (HLH) is a fatal inflammatory disease and treatments currently may lead to serious side effects. There is a pressing need for effective, less toxic treatments for this disease. Previous reports have suggested that interferon gamma (IFNgamma) has a role in the pathogenesis of HLH. Here, we report that blocking IFNgamma had a therapeutic effect in two different murine models of human hereditary HLH (perforin-deficient and Rab27a-deficient mice, both infected with lymphocytic choriomeningitis virus). Therapeutic administration of an anti-IFNgamma antibody induced recovery from haemophagocytosis in both genetic models, as evidenced by increased survival in perforin-deficient mice and correction of blood cytopenia, moderation of body temperature changes, decreased cytokinaemia, restoration of splenic architecture and reduced haemophagocytosis in the liver of both murine models. Involvement of the central nervous system in Rab27a-deficient mice was prevented by anti-IFNgamma therapy. Hepatic T-cell infiltrates and virus persisted, with no detectable harm during the time course of these studies. These data strongly suggest that neutralization of IFNgamma could be used in humans to safely alleviate the clinical manifestations of haemophagocytosis.

DOI: https://doi.org/10.1002/emmm.200900009

Neutralization of IFNγ defeats haemophagocytosis in LCMV-infected perforin- and Rab27a-deficient mice

Jana Pachlopnik Schmid[1,2,3], Chen-H. Ho[1,2], Fabrice Chrétien[4], Juliette M. Lefebvre[1,2], Gérard Pivert[5], Marie Kosco-Vilbois[6], Walter Ferlin[6], Frédéric Geissmann[5,7], Alain Fischer[1,2,3], Geneviève de Saint Basile[1,2,3]**

Keywords: haematology; haemophagocytic lymphohistiocytosis; IFNγ; immunopathology; immunotherapy

DOI 10.1002/emmm.200900009

Received August 28, 2008
Accepted January 19, 2009

Hereditary haemophagocytic lymphohistiocytosis (HLH) is a fatal inflammatory disease and treatments currently may lead to serious side effects. There is a pressing need for effective, less toxic treatments for this disease. Previous reports have suggested that interferon γ (IFNγ) has a role in the pathogenesis of HLH. Here, we report that blocking IFNγ had a therapeutic effect in two different murine models of human hereditary HLH (perforin-deficient and Rab27a-deficient mice, both infected with lymphocytic choriomeningitis virus). Therapeutic administration of an anti-IFNγ antibody induced recovery from haemophagocytosis in both genetic models, as evidenced by increased survival in perforin-deficient mice and correction of blood cytopenia, moderation of body temperature changes, decreased cytokinaemia, restoration of splenic architecture and reduced haemophagocytosis in the liver of both murine models. Involvement of the central nervous system in Rab27a-deficient mice was prevented by anti-IFNγ therapy. Hepatic T-cell infiltrates and virus persisted, with no detectable harm during the time course of these studies. These data strongly suggest that neutralization of IFNγ could be used in humans to safely alleviate the clinical manifestations of haemophagocytosis.

INTRODUCTION

Hereditary haemophagocytic lymphohistiocytosis (HLH) is a fatal inflammatory disease characterized by fever, an enlarged spleen, cytopenia, elevated blood ferritin, coagulopathy, blood lipid changes and may also lead to neurological symptoms (Henter et al, 2007). It is the consequence of hypercytokinaemia and organ infiltration by CD8-positive T-cells and macrophages and is probably caused by genetic defects that impair cell-mediated cytotoxicity, *e.g.* mutations in the genes which encode perforin, Munc13-4, syntaxin-11, the lysosomal trafficking regulator (LYST) and Rab27a (Barbosa et al, 1996; Feldmann et al, 2003; Menasche et al, 2000; Nagle et al, 1996; Perou et al, 1996; Stepp et al, 1999; zur Stadt et al, 2005). However, the same clinical syndrome can be observed in patients who do not have any of these known, inherited defects; these acquired forms of HLH can occur in patients suffering from severe infections (*e.g.* HIV and H5N1-influenza), malignancies and autoimmune, autoinflammatory or rheumatic diseases

(1) Institut National de la Santé et de la Recherche Médicale, Unité U768, Laboratoire du Développement Normal et Pathologique du Système Immunitaire, Paris, France.
(2) Université Paris Descartes, Faculté de Médecine de l'Université René Descartes, Institut Fédératif de Recherche Necker Enfants-Malades (IFR94), Paris, France.
(3) Assistance Publique-Hôpitaux de Paris, Hôpital Necker Enfants-Malades, Unité d'Immunologie et Hématologie Pédiatrique, Paris, France.
(4) Assistance Publique-Hôpitaux de Paris, Hôpital Henri Mondor, Neuropathologie, Département de Pathologie, Créteil, France.
(5) Assistance Publique-Hôpitaux de Paris, Hôpital Necker Enfants-Malades, Service d'Anatomie et de Cytologie Pathologiques, Paris, France.
(6) NovImmune SA, Geneva, Switzerland.
(7) Institut National de la Santé et de la Recherche Médicale U838, Hôpital Necker-Enfants Malades, Faculté de Médecine de l'Université René Descartes, Paris, France.
***Corresponding authors:**
Tel: +33 1 44 49 50 08; Fax: +33 1 42 73 06 40
E-mails: jana.pachlopnik@inserm.fr; genevieve.de-saint-basile@inserm.fr

(Emmenegger et al, 2005; Hsieh & Chang, 2006) and are also potentially fatal.

The only definite curative therapy for inherited forms of HLH is haematopoietic stem cell transplantation (Fischer et al, 1986). Nevertheless, about 20–25% of the patients die before transplantation due to failure of therapy or the serious side effects of the immunosuppressive (such as antithymoglobulin) and chemotherapeutic agents (such as etoposide) required to decrease hyperinflammation (Henter et al, 1997, 2007; Jordan & Filipovich, 2008; Mahlaoui et al, 2007). Removal of the infectious agent is often not sufficient, effective or rapid enough to enable recovery from HLH. Immunosuppressive/chemotherapeutic treatment must be combined with anti-infective therapy to induce remission from HLH. There is thus an overall pressing need for effective, less toxic immunosuppressive/chemotherapeutic treatments in HLH.

Several cytokines that promote HLH have been identified and are therefore candidate targets for reducing hyperinflammation. Of these various cytokines, IFNγ appears to be a promising candidate. Indeed, elevated serum IFNγ levels have been found in HLH patients (Henter et al, 1991; Mazodier et al, 2005; Nagasawa et al, 2008; Osugi et al, 1997; Takada et al, 2003) and IFNγ production was detected in the liver (Billiau et al, 2005). Elevated IFNγ levels were also found in murine models of HLH after triggering the condition by infection with lymphocytic choriomeningitis virus (LCMV) (Crozat et al, 2007; Czar et al, 2001; Jordan et al, 2004; Pachlopnik Schmid et al, 2008). It was furthermore shown that administration of anti-IFNγ antibodies to perforin-deficient mice during incubation of the LCMV infection increased survival and prevented the development of aplastic anaemia and other manifestations of HLH (Badovinac et al, 2003; Binder et al, 1998; Jordan et al, 2004).

In the present study, we looked at whether administration of an anti-IFNγ antibody would have not only a preventive but also a therapeutic effect in perforin-deficient (pfp−/−) mice with HLH as a preclinical model. Furthermore, we hypothesized that other genetic causes of HLH share a common effector pathway and therefore extended our study to the examination of Rab 27a-deficient (Rab27a−/−) mice with HLH; a murine genetic model of human Griscelli syndrome type 2.

RESULTS

Improved survival and recovery with anti-IFNγ treatment

The effects of IFNγ neutralization were tested in pfp−/− and Rab27a−/− mice that display the features of LCMV-induced HLH. After LCMV injection, pfp−/− and Rab27a−/− mice were visibly more ill than control mice, as evidenced by lethargy, scrubby fur, loss of colour in the paw pads, unstable movements, hunched back and turbid eyes appearing 7–10 days after LCMV injection. In the absence of treatment or following the administration of a control antibody, all pfp−/− mice died within 8 and 21 days after injection of 100 pfu of LCMV respectively (Fig 1A). All wild-type (wt) mice survived (data not shown). Next, 100 pfu of LCMV was injected into pfp−/− mice on day 0 and treatment with the anti-IFNγ antibody XMG1.2 was initiated on day 8, when signs of HLH (such as changes in body temperature, splenomegaly, pancytopenia, hypertriglyceridaemia and haemophagocytosis as discussed below) were first detected. Anti-IFNγ treatment (consisting of five injections, given every 3rd day from day 8 until day 20) improved survival of LCMV-infected pfp−/− mice with HLH, when compared with the control group ($p < 0.0001$). Nine out of the 11 mice in the anti-IFNγ treatment group survived. The experiment was concluded on day 27 post-LCMV injection in one group of mice (n = 3). No additional deaths occurred in the remaining mice (n = 6) observed until day 36. Anti-IFNγ antibody-treated pfp−/− mice had a better general condition, increased spontaneous locomotion, defense reactions and controlled, flowing movements when compared with the control group. One mouse within the treatment group died immediately after the first anti-IFNγ antibody injection—HLH was probably already too advanced. Another mouse within the treatment group died on day 15 after LCMV injection and showed a haemorrhagic abdominal cavity—probably as a consequence of traumatic bleeding caused by the injection of anti-IFNγ antibody on day 14. Following LCMV injection, wt mice stopped gaining body weight, while pfp−/− mice lost body weight. Weight loss was attenuated by anti-IFNγ antibody treatment in pfp−/− mice (Fig 1B). The mice were febrile on day 6 (Fig 1C). Wt mice had normal to slightly elevated body temperatures thereafter, whereas pfp−/− mice developed hypothermia. Hypothermia was controlled by anti-IFNγ treatment (Fig 1C).

Although Rab27a−/− mice were visibly ill after LCMV injection, mortality was observed in only one out of five untreated mice and zero out of five control antibody-treated mice (Fig 1D). Survival in anti-IFNγ-treated mice (n = 5) was 100%. Treatment consisted of four injections, given every 3rd day from day 13 until day 22 after LCMV injection. The experiment was concluded on day 25 post-LCMV injection in one group of mice (n = 8, with four anti-IFNγ-treated and four control antibody-treated animals). No additional deaths occurred in the remaining mice (n = 6) observed until day 34. Another group of mice (n = 4, with two anti-IFNγ-treated and two control antibody-treated animals) was observed until day 70 and no deaths occurred in this group. Given the survival of infected, untreated Rab27a−/− mice with HLH, we considered that this mouse model was useful for studying differences between treatment and control groups in more phenotypic detail. In Rab27a−/− mice, anti-IFNγ treatment improved the general clinical condition (data not shown) and attenuated weight loss, when compared with control antibody treatment (Fig 1E). Hypothermia in Rab27a−/−mice was reduced by anti-IFNγ, when compared with control antibody treatment (Fig 1F). The clinical condition of untreated (data not shown) and control antibody-treated Rab27a−/− mice improved spontaneously, so that there was no significant difference in body weight from day 40 and in body temperature from day 25 post-LCMV injection onwards, when compared with anti-IFNγ-treated mice.

Improved haematological parameters with anti-IFNγ treatment

A drop in the haemoglobin level, neutrophil and thrombocyte counts is one of the major features in human HLH. We, therefore, analysed these parameters in mice before and during anti-IFNγ treatment. Although anaemia and thrombocytopenia were found in all animals (*i.e.* wt, pfp−/−, Rab27+/− and Rab27a−/− mice) on day 8 after LCMV injection, these parameters were significantly lower in pfp−/− and Rab27a−/− mice than in the controls (Fig 1G and data not shown). Absolute neutrophil counts decreased slightly in pfp−/− and Rab27a−/− mice, while an increase was observed in wt mice on day 8 after LCMV injection. All parameters improved in pfp−/− mice on anti-IFNγ treatment and returned to normal levels two to three weeks after therapy initiation, whereas control antibody-treated pfp−/− mice succumbed at the nadir. Given that Rab27a−/− mice with HLH survived even in the absence of treatment, it was possible to compare the respective blood counts for anti-IFNγ- and control antibody-treated mice for a longer period of time. Blood cell counts increased during anti-IFNγ treatment, while pancytopenia persisted in control antibody-treated mice (Fig 1H).

Histopathological features of bone marrow and spleen during anti-IFNγ treatment

The positive effect of anti-IFNγ treatment on haematopoiesis was also visible in bone marrow sections of pfp−/− and Rab27a−/− mice and through the presence of an increased red cell distribution width, which is a parameter of active erythropoiesis (Fig 2A and B and data not shown). Splenomegaly is one of the diagnostic criteria for human HLH. We, therefore, analysed spleen weight in mice during HLH and the subsequent anti-IFNγ treatment. However, spleen size may not be a fully accurate parameter for murine HLH for several reasons. Firstly, in contrast to human, mouse spleens continue to function as a haematopoietic organ in postnatal life. This could have an impact on the spleen size as a readout criterion in a disease like HLH, where active haematopoiesis is a sign of recovery. Secondly, spleen size in pfp−/− mice did not correlate with disease severity, since spleens in LCMV-infected pfp−/− mice with HLH were not significantly enlarged when compared with LCMV-infected wt mice (Fig S1A of Supporting Information). Thirdly, spleen size in pfp−/− mice tended to correlate with the LCMV dose administered (Pearson r = 0.9) (Fig S1B of Supporting Information). In Rab27a−/− mice, spleen size was substantially increased on day 13 post-LCMV injection, *i.e.* prior to any antibody treatment (Fig S1C of Supporting Information). Spleen size tended to decrease in anti-IFNγ-treated Rab27a−/− mice, whereas there was no significant change in control antibody-treated mice. The anatomical structure of the spleen was markedly modified by HLH. The red pulp was enlarged and the white pulp was disorganized (Fig 2C and D). Interestingly, anti-IFNγ antibody treatment almost completely normalized the

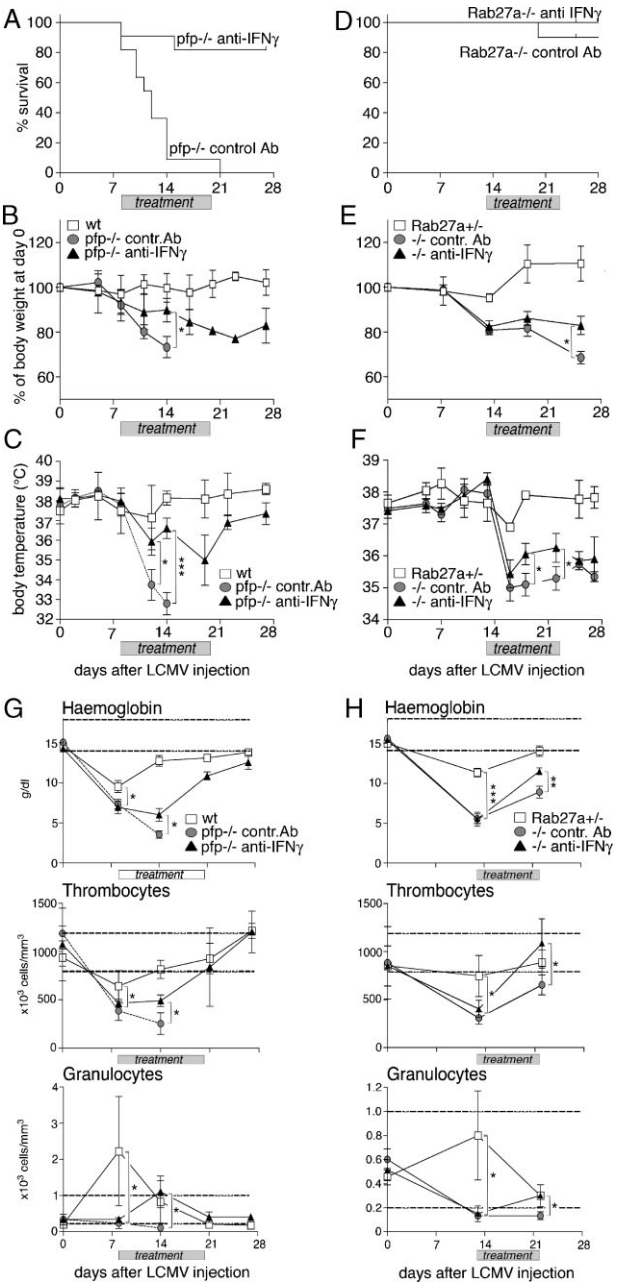

Figure 1. Anti-IFNγ treatment improves survival and clinical as well as haematological recovery. In the panels on the left-hand side, data from pfp−/− mice are shown that were injected with LCMV (100 pfu) on day 0 and treated either with anti-IFNγ or with control antibodies from day 8 to day 20 (five injections); in the panels on the right-hand side, data from Rab27a−/− mice are shown that were injected with LCMV (500 pfu) on day 0 and treated either with anti-IFNγ or with control antibody from day 13 to day 22 (four injections); open squares indicate control mice (wt and Rab27a+/−), black triangles mice treated with anti-IFNγ (pfp−/− and Rab27a−/−) and grey dots mice treated with control antibody (pfp−/− and Rab27a−/−).

A–C. (A) Survival, (B) body weight and (C) body temperature of pfp−/− mice.

D–F. (D) Survival, (E) body weight and (F) body temperature of Rab27a−/− mice.

G. Blood haemoglobin level and thrombocyte and neutrophilic granulocyte counts in pfp−/− mice.

H. Blood haemoglobin level and thrombocyte and neutrophilic granulocyte counts in Rab27a−/− mice. The dashed lines in (G) and (H) correspond to normal values in C57BL/6J wt mice given in the book by Metcalf (2005). Blood counts are representative for two independent experiments; $^{*}p < 0.05$; $^{**}p < 0.005$, $^{***}p < 0.001$.

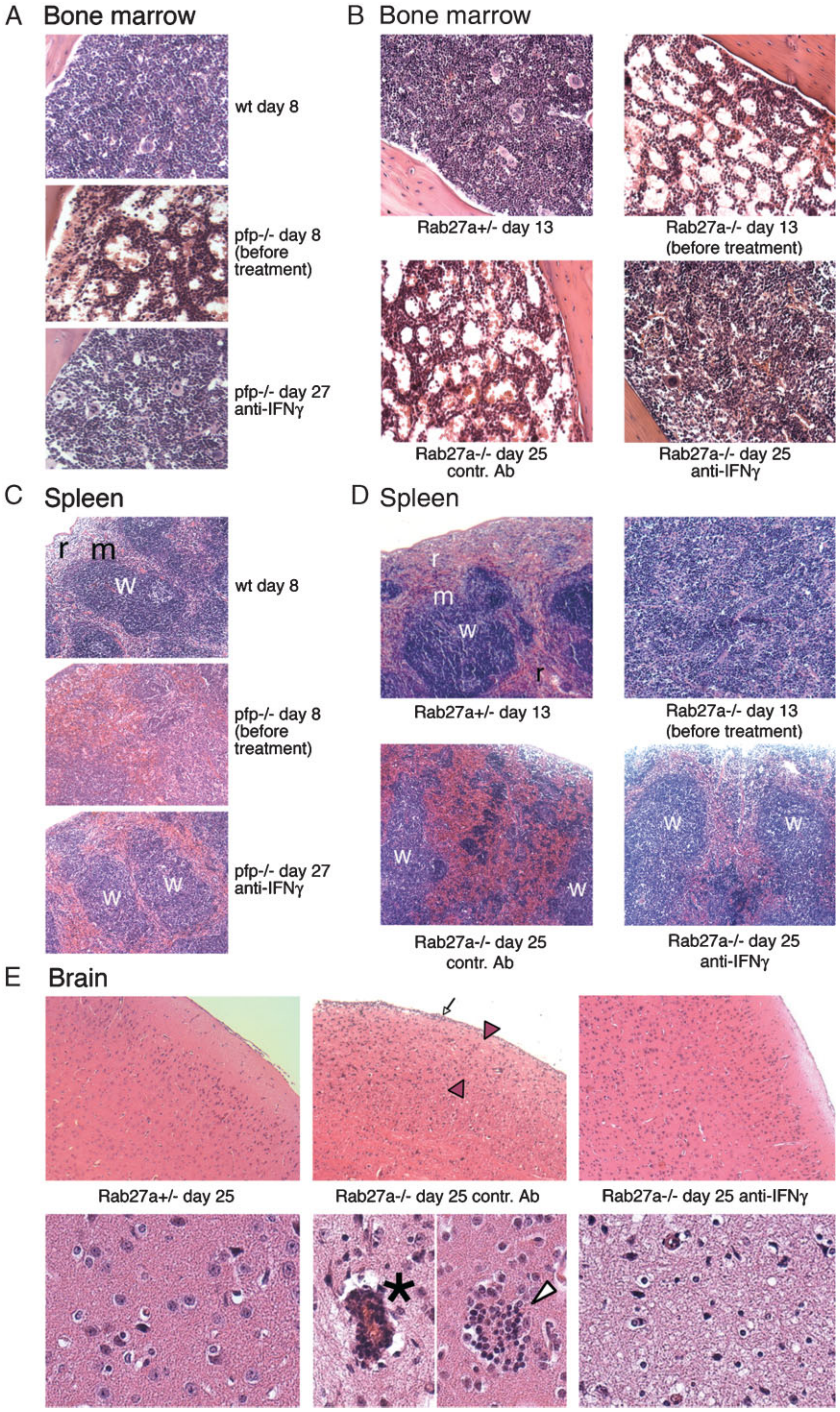

Figure 2. Histopathological features of bone marrow, spleen and brain before and after anti-IFNγ treatment.

A, B. Bone marrow sections of the right femur from (A) wt and pfp−/− mice and (B) Rab27a+/− and Rab27a−/− mice at different times after LCMV-injection, without any antibody treatment, after treatment with control or with anti-IFNγ antibody; treatment schedules were the same as indicated for Fig 1; 25× objective lens.

C. Spleen sections from wt and pfp−/− mice at different times after LCMV-injection, without any antibody treatment or after treatment with anti-IFNγ antibody (r = red pulp, m = marginal zone and w = white pulp).

D. Spleen sections from a Rab27a+/− and Rab27a−/− mice at different times after LCMV-injection, without any antibody treatment, after treatment with control or with anti-IFNγ antibody (r = red pulp, m = marginal zone and w = white pulp); 10× objective lens.

E. *Left panels*: Brain sections showing parenchyma with discrete lymphocytic infiltrates in a Rab27a+/− mouse; *Middle panels*: a diffuse lymphocytic infiltrate in the subcortical region (red arrowheads), meningitis (arrow), a perivascular cuff (asterix) and an intraparenchymal lymphocytic cluster (white arrowhead) in a Rab27a−/− mouse after control antibody treatment; *Right panels*: discrete lymphocytic infiltrates in a Rab27a−/− mouse after anti-IFNγ treatment, all analysed on day 25 after LCMV injection; *Upper panels*: 25× objective lens, lower panels: 100× objective lens. Representative histological sections stained with haematoxylin and eosin are shown.

anatomical structure in both, pfp−/− and Rab27a−/− mice, with restoration of the white pulp's initial condition.

Attenuated development of cerebral infiltrates during anti-IFNγ treatment

Involvement of the central nervous system (CNS) is one of the major concerns in human HLH. We, therefore, analysed cerebral histopathology in mice with HLH after anti-IFNγ treatment. Cerebral histopathological changes were not present in Rab27a−/− before anti-IFNγ treatment on day 13 after LCMV injection (data not shown). However, diffuse lymphocyte infiltrations, intraparenchymal lymphocytic accumulation and perivascular (pericapillar) cuffs were present in Rab27a−/− mice at day 25 after control antibody treatment (Fig 2E) and consisted of Granzyme B positive CD8 T-cells (data not shown). In contrast, there were no intraparenchymal lymphocytic

clusters and no signs of vasculitis in anti-IFNγ treated mice. Thus, cerebral histopathological changes that developed in Rab27a−/− mice treated with control antibody were prevented by anti-IFNγ treatment.

Neutralization of IFNγ

IFNγ serum levels were increased in pfp−/− and Rab27a−/− mice on day 8, whereas wt and Rab27a+/− mice showed only a moderate peak on day 6 after LCMV infection (Fig 3A and B). Some of the control antibody-treated pfp−/− mice died at the IFNγ peak, while the others died once the IFNγ serum level had decreased. Surprisingly, a delayed decrease in IFNγ serum levels was observed in mice treated with anti-IFNγ antibodies. This effect could have resulted from the formation of immune complexes between IFNγ and the anti-IFNγ antibody. Such complexes were indeed detected in the serum of these animals (Fig 3C). At later time points after antibody treatment, IFNγ was no longer detectable (data not shown). Immune complex formation probably increased the half-life of IFNγ and we, therefore, analysed whether IFNγ was biologically active. Quantification of inducibly expressed GTPase (IGTP) transcription in the macrophage cell line RAW264.7 is a reliable test to measure the biological activity of IFNγ since its transcript levels strikingly correlated with IFNγ concentrations as evidenced in Fig S2 of Supporting Information. The serum-induced IGTP transcript level was considerably reduced, reaching control value, on using serum of anti-IFNγ treated mice compared to serum of untreated mice (Fig 3D and E). Thus, anti-IFNγ treatment was effective in inhibiting the biological activity of IFNγ.

Cytokine levels in anti-IFNγ-treated pfp−/− and Rab27a−/− LCMV-infected mice

In order to establish whether or not the biological activity of IFNγ had been neutralized *in vivo*, we measured serum levels of tumour necrosis factor (TNF)-α, granulocyte monocyte colony stimulating factor (GM-CSF) and interleukin (IL)-12p70 in pfp−/− and Rab27a−/− mice during anti-IFNγ treatment (Fig 3F and G). Serum levels of TNF-α were found to be lower in anti-IFNγ treated compared to control antibody treated mice in both murine models. GM-CSF levels were also lower in anti-IFNγ treated compared to control antibody treated mice, however a significant difference was solely observed in Rab27a−/− mice. Similarly, IL-12p70 levels decreased upon anti-IFNγ treatment. The high mortality of control antibody treated pfp−/− mice impaired cytokine measurements at late time points. However, during anti-IFNγ treatment, there was no significant difference in the serum levels of chemokine ligand 5 (CCL5), a chemokine mostly secreted by activated T-cells. IL-17 levels showed a tendency to increase in anti-IFNγ-treated pfp−/− and Rab27a−/− mice when compared with control antibody treated mice. However, the difference in IL-17 levels between control antibody- and anti-IFNγ-treated mice was not significant, the levels varied strongly from mouse to mouse and did not exceed the levels found in LCMV-infected Rab27a+/− control mice that did not receive any antibody treatment. Furthermore, this slight increase in IL-17 was transient and the mice did not show any sign of autoimmunity during this time (data not shown).

Reduced macrophage activation in the liver during anti-IFNγ treatment

Given that macrophage activation is one of the hallmarks of HLH, we analysed the morphology of macrophages in tissue sections of LCMV-infected Rab27a−/− mice. Macrophages were activated (as assessed by increase in size and engulfment of other blood cells, *i.e.* haemophagocytosis) in liver sections of pfp−/− and Rab27a−/− mice before antibody-treatment and in Rab27a−/− mice during control antibody treatment, when compared with control (wt and Rab27a+/−) mice (Fig 4A and B). Liver sections in control mice contained Kupffer cells, the liver's resident macrophages. Anti-IFNγ treatment reduced macrophage activation, as evidenced by fewer activated macrophages with haemophagocytosis in histological sections in both, LCMV-infected pfp−/− and Rab27a−/− mice, compared with mice prior to any antibody treatment and those treated with control antibody (Fig 4A and B and Table 1). Triglyceride and ferritin levels, further parameters of HLH, were also found to be increased in pfp−/− and Rab27a−/− mice before antibody treatment when compared to control mice (Fig 4C–F). A significant reduction in triglyceride and ferritin levels was observed over time.

Persistence of virus in anti-IFNγ-treated mice

Because of the genetic defect in cytotoxicity, LCMV persisted in both pfp−/− and Rab27a−/− mice. Given that IFNγ neutralization is immunosuppressive, we compared the viral load in anti-IFNγ and control antibody-treated mice to assess the effect on virus replication control. There was no consistent association of the viral load with anti-IFNγ treatment since there was neither a difference in viral load between anti-IFNγ and control antibody treated Rab27a−/− mice nor an increase in viral load in anti-IFNγ treated mice when compared with mice before treatment in both murine models, pfp−/− and Rab27a−/− mice (Fig 5A and B). Viral persistence in the liver was also visualized by immunohistochemical analyses. Viral antigen was detected in periportal infiltrates in the vicinity of CD3 and Granzyme B positive cells. Similar infiltrates were observed in all three groups, anti-IFNγ treated pfp−/− mice, anti-IFNγ and control antibody-treated Rab27a−/− mice (Fig 5C, Fig S3 of Supporting Information and data not shown). Despite persistence of virus and periportal infiltrates, serum aspartate-aminotransferase levels (a measure of liver pathology) did not increase over time (Fig 5D and E). Taken as a whole, our results show that anti-IFNγ therapy reduced the consequences of macrophage activation but did not have any consistent influence on the LCMV load, at least during the course of treatment used in this study.

DISCUSSION

We treated perforin-deficient mice and Rab27a-deficient mice suffering from LCMV-induced HLH with either anti-IFNγ or control antibodies. Our study demonstrated that anti-IFNγ antibody treatment had a marked therapeutic effect on HLH in both models. LCMV-infected perforin- and Rab27a-deficient mice developed pancytopenia, splenomegaly, body temperature changes, hypercytokinaemia and histopathological features

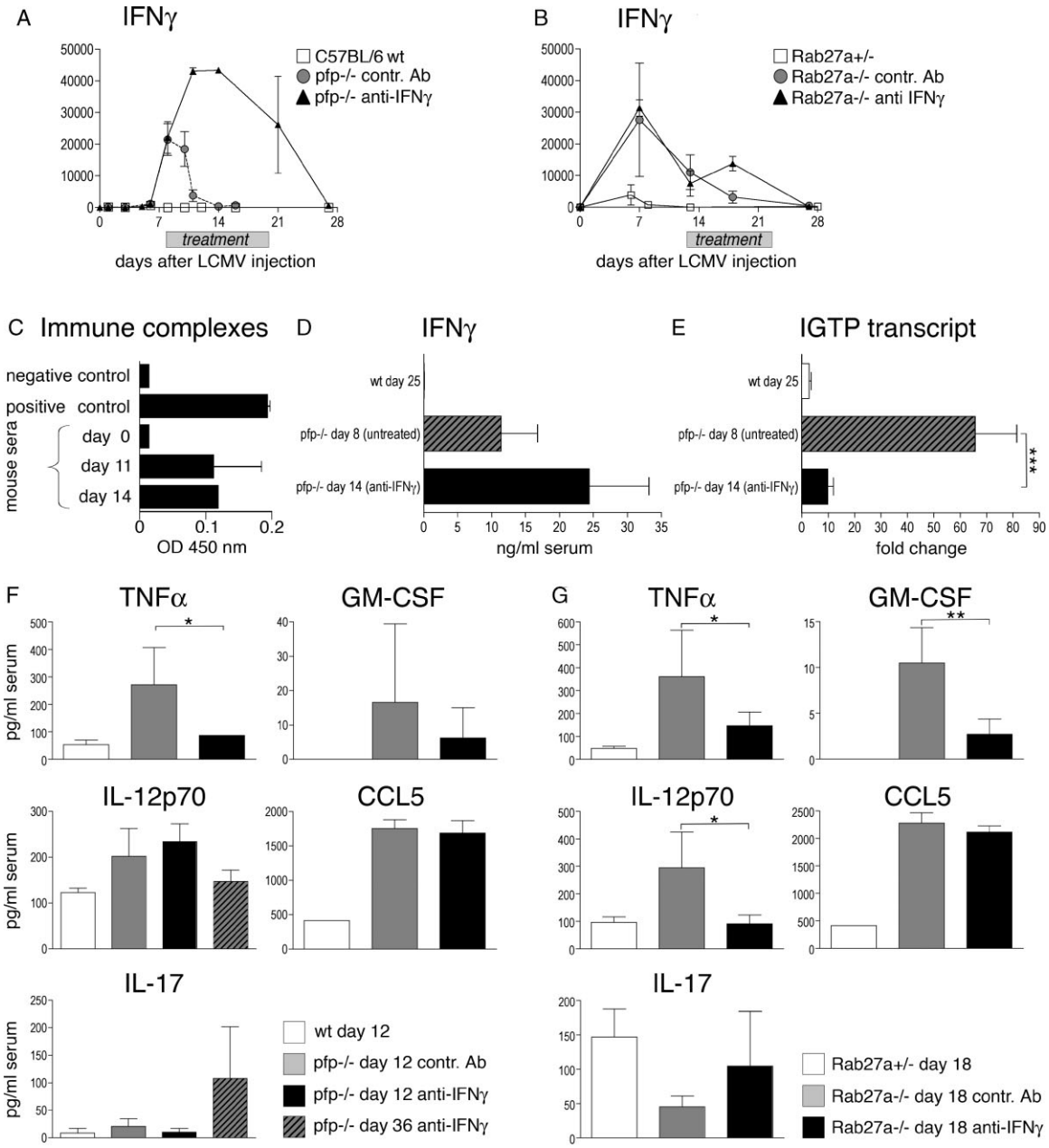

Figure 3. Neutralization of IFNγ and decrease of macrophage derived cytokine levels with anti-IFNγ treatment.

A, B. IFNγ serum levels in (A) pfp−/− and (B) Rab27a−/− mice at various times after LCMV injection, as determined by ELISA. LCMV injections and antibody treatments in all experiments were performed as indicated in Fig 1. Open squares indicate serum levels in wt (or Rab27a+/−) mice; grey dots, pfp−/− (or Rab27a−/−) mice treated with control antibody; black triangles, pfp−/− (or Rab27a−/−) mice treated with anti-IFNγ antibody. Values represent mean ± standard error of the mean (SEM) ($n \geq 3$ per group) and are representative for two independent experiments.

C. Serum levels of immune complexes of rat IgG and mouse IFNγ in pfp−/− mice. Serum levels of immune complexes were measured on days 0, 11 and 14 by ELISA with goat anti-rat IgG as capture antibody and goat anti-mouse IFNγ as revealing antibody. Dilution buffer was used as a negative control and rat anti-mouse IFNγ that was pre-incubated with mouse IFNγ was used as a positive control. Values represent mean+SD of duplicate measurements ($n = 3$ per group).

D. IFNγ serum levels of pfp−/− mice on day 8 (*i.e.* before anti-IFNγ) and day 14 (*i.e.* during anti-IFNγ treatment) as determined by ELISA.

E. Serum-induced IGTP transcript levels in RAW264.7 cells by the same serum samples as in (D), measured by quantitative RT-PCR. The data show the fold difference in the IGTP-transcript compared to stimulation with cell culture medium alone. Values represent mean ± SEM ($n = 5$ per group from two independent experiments).

F, G. Serum levels of TNF-α, GM-CSF, IL-12p70, CCL5 and IL-17 in (F) pfp−/− mice on day 12 (or day 36) and in (G) Rab27a−/− mice on day 18 after LCMV-injection treated with control or anti-IFNγ antibody, measured by Multiplex cytokine assay. Values represent mean +SD ($n \geq 3$ per group) and are representative of two independent experiments. White bars indicate measurements in wt (or Rab27a+/−) mice, grey bars pfp−/− (or Rab27a−/−) mice treated with control antibody and black bars pfp−/− (or Rab27a−/−) mice treated with anti-IFNγ antibody. $^{*}p < 0.05$, $^{**}p < 0.005$, $^{***}p < 0.001$.

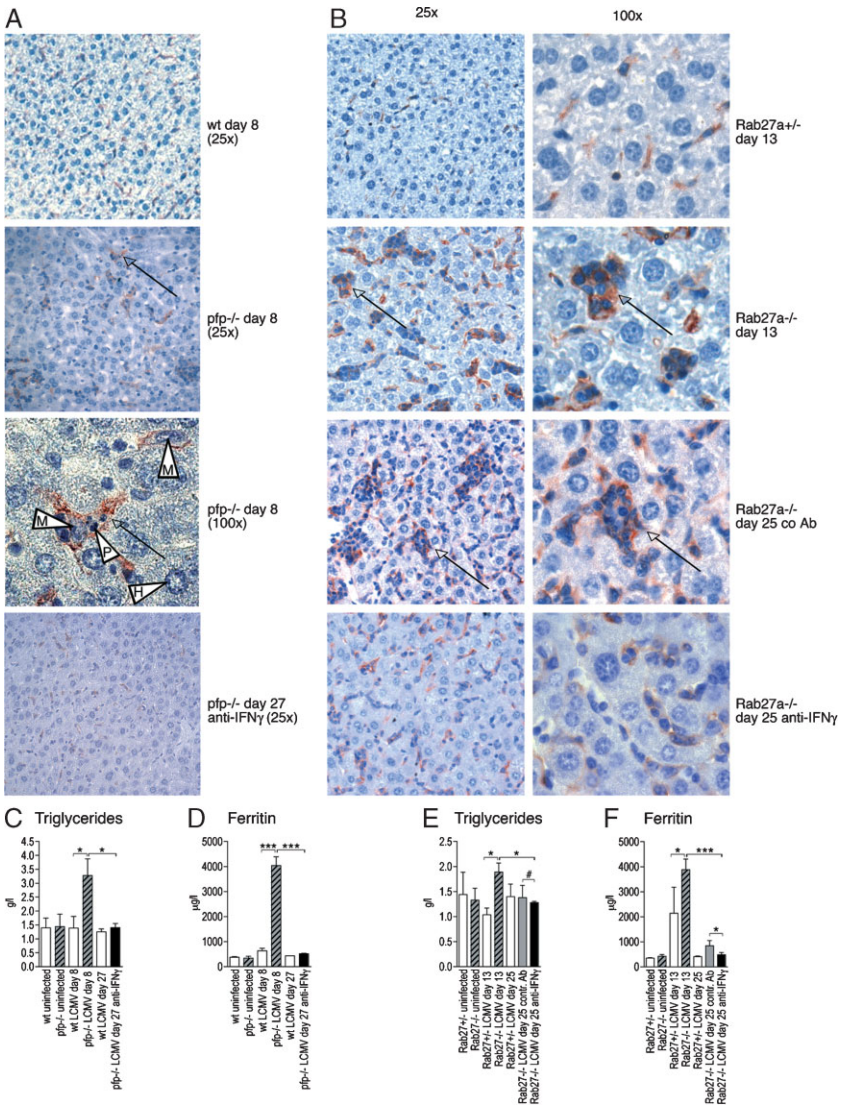

Figure 4. Reduced macrophage activation after anti-IFNγ treatment.

A, B. Liver sections stained with anti-macrophage antibody F4/80 in (A) wt and pfp−/− mice and in (B) Rab27a+/− and Rab27a−/− mice at different times after LCMV-injection, without any antibody treatment, after treatment with control or with anti-IFNγ antibody; treatment schedules were the same as indicated for Fig 1; arrows indicate the corresponding cells at different magnifications; arrowheads indicate: H = nucleus of hepatocyte, M = nucleus of macrophage, *p* = phagocytosed cell, M + P indicating haemophagocytosis; 25× and 100× objective lens as indicated.

C, E. Serum triglyceride levels in (C) pfp−/− and (E) Rab 27a−/− mice.

D, F. Serum ferritin levels in (D) pfp−/− and (F) Rab 27a−/− mice. Mean + SD of measurements ($n \geq 4$ per group). $^{\#}p > 0.05$, $^{*}p < 0.05$, $^{***}p < 0.001$.

Table 1. Quantification of haemophagocytosis in liver sections

	Number of macrophages with haemophagocytosis					
	pfp−/−			Rab27a−/−		
Day after LCMV injection	8	27	*p*	18–25	18–25	*p*
Antibody treatment	No	Anti-IFNγ		Control Ab	Anti-IFNγ	
Mean ± SEM[1]	249.9 ± 23.6	44.8 ± 5.3	<0.0001	102.9 ± 8.4	63.7 ± 7.2	0.0010

Quantification of macrophages with engulfed blood cells. Histological analysis of liver sections was performed on ten visual fields (10× objective lens) per mouse with two mice per group, with each visual field subdivided into 20 quadrants. The number of macrophages with haemophagocytosis was counted in at least 100 representative quadrants per mouse. The number of macrophages with haemophagocytosis is expressed as the count per 100 quadrants.
[1]mean number of macrophages with engulfed cells per 100 quadrants ± standard error of the mean (SEM).

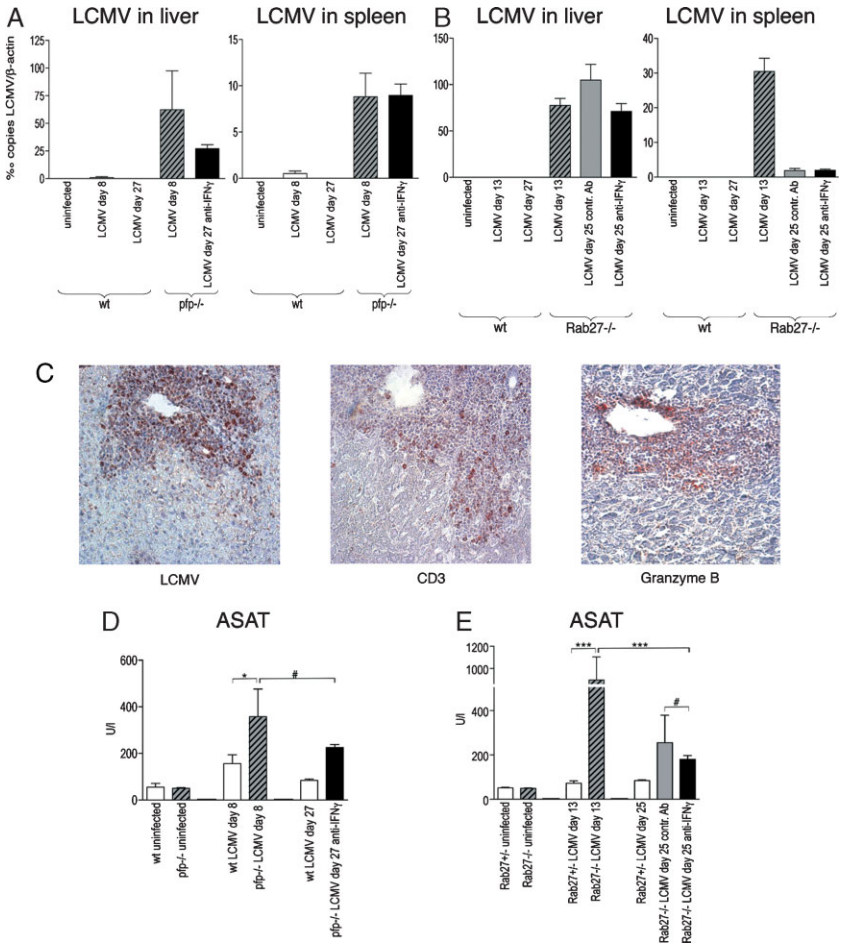

Figure 5. Persistence of virus and lymphocytes in the liver of anti-IFNγ-treated mice.

A, B. Viral load in livers and spleens of (A) pfp−/− and (B) Rab27a−/− mice as measured by quantitative PCR, expressed as number of LCMV-copies per mill β-actin-copies. Measurements in (A) were performed on day 0, 8 and 27, in (B) on day 0, 13 and 25 after LCMV-injection. Striped bars indicate measurements in LCMV-infected mice before any antibody treatment, black bars mice treated with anti-IFNγ antibody and grey bars Rab27a−/−mice treated with control antibody. Values represent mean + SD from two independent experiments.

C. Infiltration in the portal tract of liver sections stained with antibodies to LCMV (left panel), CD3 (middle panel) and Granzyme B (right panel) from a pfp−/− mouse that was treated with anti-IFNγ antibody from day 8 to day 20 and analysed on day 27 after LCMV injection; 25× objective lens. Images are also representative for immunohistochemical stainings in Rab27a−/− under anti-IFNγ as well as under control antibody treatment.

D, E. Aspartate aminotransferase (ASAT) levels in the serum of (D) pfp−/− and (E) Rab27a−/− mice before and after LCMV-injection, receiving anti-IFNγ or control antibody treatment. Values represent mean + SD (n = 4 per group); LCMV injections and antibody treatments in all experiments were performed as indicated in Fig 1. $^{\#}p > 0.05$, $^{*}p < 0.05$, $^{***}p < 0.001$.

characteristic of HLH (such as bone marrow hypoplasia, disturbance in splenic architecture and haemophagocytosis). This is consistent with previous studies of perforin- and Rab27a-deficient mice (Binder et al, 1998; Jordan et al, 2004; Pachlopnik Schmid et al, 2008) and confirms that these mice represent reliable models of human HLH. A prime role of IFNγ in the pathogenesis of haemophagocytosis has been shown; secondary prevention by anti-IFNγ antibodies increased the survival rate and had a preventive effect on the development of aplastic anaemia and other signs of HLH in perforin-deficient mice (Badovinac et al, 2003; Binder et al, 1998; Jordan et al, 2004). Herein, we show that delayed administration of an IFNγ-neutralizing antibody led to recovery from HLH in perforin- and Rab27a-deficient mice, based on prevention of death in perforin-deficient mice and the correction of pancytopenia, moderation of weight loss and hypothermia, reduction of macrophage-dependent cytokinaemia, restoration of splenic architecture and reduction of haemophagocytosis in the liver of both murine models. Thus, we achieved a therapeutic, not only a preventive, effect. CNS affection is a major concern in HLH and has a significant impact on the long-term outcome of the patients. The effect of IFNγ neutralization on CNS involvement has not been investigated so far in HLH. We show that in HLH anti-IFNγ therapy has a beneficial effect on CNS lymphocytic infiltration. HLH was less fatal in the Rab27a-deficient mice than in the perforin-deficient animals, since most of the former survived HLH in the absence of IFNγ neutralization. This is reminiscent of the respective human conditions, since disease onset occurs later in patients with nonsense mutations in Rab27a (Griscelli syndrome type 2) than in those with nonsense mutations in perforin (familial HLH type 2) (Feldmann et al, 2002; Horne et al, 2008; Mamishi et al, 2008). Furthermore, NK cells derived from patients with Griscelli syndrome type 2 exhibit residual cytotoxicity (Gazit et al, 2007; Plebani et al, 2000).

Our results demonstrate that the pathophysiology of HLH can be divided into two steps: (i) virus-triggered CD8 T-cell activation/expansion that results in high, sustained production of IFNγ in the absence of virus clearance and (ii) IFNγ-mediated macrophage activation. Only the second step is inhibited by the anti-IFNγ antibody. It is worth emphasizing that this is enough to enable survival of LCMV-infected, perforin-deficient mice with HLH and to alleviate most of the HLH symptoms in perforin- and Rab27a-deficient mice. These results highlight the central role of IFNγ-driven macrophage activation in HLH, defining this condition as a unique pathophysiological entity. Apparently, there is a significant prevention of T-lymphocytic

infiltrates in the brain during anti-IFNγ therapy. This contrasts with a persistence of hepatic T-cell infiltrates in the treated animals. This difference might be explained by the hepatotropic nature of the LCMV strain in this study. Another explanation could be an anti-inflammatory effect of the anti-IFNγ therapy, which by reducing the production of macrophage-derived cytokines might help to normalize the blood–brain barrier tightness (Abbott et al, 2006; Polavarapu et al, 2005).

Delayed clearance of IFNγ in perforin- and Rab27a-deficient mice receiving anti-IFNγ treatment may be explained by the formation of immune complexes between IFNγ and anti-IFNγ antibodies. Previous studies have shown that other antibodies used as therapeutic agents may also increase the half-life of their antigen, even though these antibodies neutralize the biological activity of the latter (Corne et al, 1997; Lainee et al, 2005; Rojas et al, 2005). Such immune complexes do not appear to be detrimental to the hosts.

Perforin-deficient mice not treated with anti-IFNγ succumbed soon after disease onset. Thus, the treatment had to be initiated early on in the time-course of the active disease. In contrast, most Rab27a-deficient mice survived LCMV-induced HLH—even in the absence of IFNγ neutralization. Therefore, the Rab27a-deficient mouse model provided us with an opportunity to study the effect of anti-IFNγ antibody at a later stage in HLH and compare it with a control antibody treatment group. In addition, the Rab27a-deficient model makes it possible to clearly distinguish HLH-associated phenomena from perimortem events. Even though anti-IFNγ treatment was started late (day 13) in disease progression, a remarkable therapeutic effect was equally observed in Rab27a-deficient mice when compared with perforin-deficient mice treated early in the course of the disease.

This study shows that anti-IFNγ treatment induces recovery from HLH, despite viral persistence. Although the general condition of perforin- and Rab27a-deficient mice with HLH clearly improved during treatment with anti-IFNγ antibodies, the treated mice were not completely healthy and did not regain full body weight, compared with non-infected littermates. The treated mice showed persistent periportal T-cell infiltrates in the liver. The location of these infiltrates was very similar to that observed in LCMV-infected IFNγ−/− mice and in other types of chronic viral hepatitis (Kunar et al, 2005; Moskophidis et al, 1994; Nansen et al, 1999). We show that these T-cell infiltrates were associated locally with areas of LCMV detection —strongly suggesting the presence of active, LCMV-driven T-cell responses. Thus, the incomplete recovery of the mice with LCMV-triggered HLH that had been treated with anti-IFNγ antibodies can probably be explained by viral persistence. It is likely that insufficient cytotoxicity (due to the perforin- or Rab27a-deficiency) impaired the killing of infected cells and thereby enabled viral persistence. Although neutralization of IFNγ *per se* might have compromised virus control (Moskophidis et al, 1994; Nansen et al, 1999), it had no detectable effect on the viral load.

In view of the efficacy shown in the present study, we suggest that IFNγ neutralization could be useful for reducing the signs of HLH in patients. This conclusion is supported by the striking similarity between HLH occurring in humans and in relevant animal models, as shown here and in Unc13-d (the mouse orthologue of human Munc13-4)-deficient mice (Crozat et al, 2007) by the substantially elevated serum IFNγ levels in murine HLH. Patients with inherited and acquired HLH have very high IFNγ serum levels during the active disease (Henter et al, 1991; Mazodier et al, 2005; Nagasawa et al, 2008; Osugi et al, 1997; Takada et al, 2003 and our own unpublished observations). An anti-human IFNγ antibody (fontolizumab) has been shown to be safe in clinical trials in Crohn's disease (Hommes et al, 2006; Reinisch et al, 2006). In addition, fontolizumab's therapeutic effects have been documented in patients with inflammatory skin diseases and in a clinical trial of patients with corneal transplant rejection (Skurkovich et al, 2002; Skurkovich & Skurkovich, 2005). The patient numbers might not be large enough to draw any firm conclusions on any infectious, neoplastic and allergic complications potentially attributable to fontolizumab. However, the effect of neutralizing IFNγ on the response to infection is probably minor for a short period of therapy. Indeed, patients with inborn errors of the IL-12/23-IFNγ loop display normal resistance to most infections, with the notable exception of mycobacteria and, in some cases, *Salmonella* (Mansouri et al, 2005). However, such infections require a persistent defect in the IL-12/23-IFNγ loop. It is also noteworthy that delayed neutralization of IFNγ improved survival rates and attenuated organ dysfunctions in a primate model of bacteriaemic shock (Lainee et al, 2005).

Alternatively, this treatment could be especially attractive in patients with hereditary HLH, given that current drugs such as etoposide (Henter et al, 2007) or antithymoglobulin (Mahlaoui et al, 2007) can be toxic and are far more immunosuppressive than a transient IFNγ blockade. Another potential advantage of an IFNγ blockade in the management of inherited HLH might be its ability to improve engraftment in haematopoietic stem cell transplantation (Rottman et al, 2008), the curative step in the therapy of inherited HLH. Neutralization of IFNγ might also be an efficient and safe way to treat patients with acquired HLH (acquired HLH has been observed notably in severe infections, malignancies, autoimmune, autoinflammatory and rheumatic diseases) (Emmenegger et al, 2005; Hsieh & Chang, 2006), provided that the T-cell activation trigger is also amenable to therapy.

In conclusion, the present study shows that treatment of HLH with IFNγ-blocking antibodies induces recovery and improves survival rates in two different murine models, despite the persistence of the initial infectious trigger. In view of the fact that humanized anti-IFNγ antibodies are reportedly safe in clinical trials of other diseases, further investigation is warranted in order to determine their potential clinical efficacy in hereditary and acquired forms of HLH.

MATERIALS AND METHODS

Mice

C57BL/6J wt, C57BL/6J-Prf1^{tm1Sdz}/J (herein after referred to as pfp−/−) and C3H/HeSn-Rab27a^{ash}/J (so-called *ashen* mice) were purchased from the Jackson Laboratory. C57BL/6J-Rab27a ^{ash}/j (Rab27a−/−) mice were obtained by backcrossing C3H/HeSn-Rab27a^{ash}/J with C57BL/6J wt mice for 10 generations. For experiments with Rab27a−/− mice,

the offspring of a heterozygous X homozygous crossing were used. Heterozygous offspring were used as controls in the experiments with Rab27a−/− mice. Mice were maintained and handled in accordance with the national and institutional polices. The study protocol was approved by the local ethics committee. Body temperature was measured using a rodent rectal thermometer (BIOSEB).

The presence of the Rab27a-mutation was verified by restriction site analysis of polymerase chain reaction (PCR) products of mouse tail DNA. Briefly, 0.5 cm from the end of a mouse's tail was incubated at 37°C in lysis buffer (50 mM Tris-Cl pH 8.0, 100 mM EDTA, 100 mM NaCl, 1% SDS) containing proteinase K (0.7 mg/ml) overnight. DNA was extracted thereafter using phenol/chloroform. PCR was performed using the following primers: forward: 5′-CTTTCTCTTCCACCATACTT-3′ and reverse: 5′-AAGCGAGTTCCAGGGCAG-3′. The PCR products were purified using a PCR Purification Kit (QIAGEN), restricted by RsaI at 37°C for 4 h and then separated on a 2% agarose gel containing ethidium bromide. DNA from Rab27a−/− mice produced a single, 534 bp band, DNA from wt mice produced a 242 bp band and a 291 bp band and DNA from heterozygous mice resulted in three bands with 534, 291 and 242 bp, respectively.

Viral preparations

LCMV WE (Battegay et al, 1991), kindly provided by Professor Maries van den Broek and Professor Rolf Zinkernagel (University of Zürich, Switzerland), was injected intraperitoneally to 6–8 weeks old pfp−/− and 6–14 weeks old Rab27a−/− mice. Infected animals and biological material potentially containing LCMV were handled in a Biosafety Level 2 environment.

Treatment schedules

In pfp−/− mice and their wt controls, 100 pfu of LCMV were injected on day 0 and treatment with anti-IFNγ antibodies was initiated on day 8. This viral dose was chosen because it induced mortality in 100% of pfp−/− mice, while the treatment time was chosen because the mice then showed multiple features of HLH (thus enabling assessment of a potential therapeutic effect of the anti-IFNγ antibody injections). It should be noted that some of the mice already succumbed at this time. There were no significant differences between infected, untreated ($n = 7$) and infected, control antibody-treated ($n = 4$) pfp−/− mice in terms of any of the tested parameters and so the two groups were pooled. Rab27a−/− mice and their heterozygous controls received a dose of 500 pfu of LCMV on day 0. This dose was chosen because it resulted in the highest serum IFNγ-levels, compared with mice that had received a higher (1×10^4 pfu) or a lower (100 pfu) viral dose (data not shown). The treat-ment with anti-IFNγ antibodies in Rab27a−/− mice was started later than in pfp−/− mice (namely on day 13 after LCMV injection) because we sought to initiate treatment as late as possible during the active phase of HLH, in order to better assess the effect of anti-IFNγ therapy. The data shown are representative of 2–7 independent experiments.

Blood counts and ferritin

Blood counts were determined using the MS 9-5V automated cell counter (Melet Schloesing Laboratories). For ethical reasons, consecutive blood samples from the same animals were taken from the tail vein instead of the orbital cavity. This has to be taken into account when comparing blood counts presented here with those from other studies. Ferritin levels were determined using an enzyme-linked immunosorbent assay (ELISA) kit (ALPCO Diagnostics).

Cytokine measurements and antibodies

IFNγ levels in mouse sera were determined using ELISA kits (R&D Systems), the other cytokine serum levels by a BioPlex custom-mixed immunoassay panel run on a BioPlex 200 System and analysed using BioPlex Manager software (version 4.1, BioRad Laboratories). Immune complexes were detected by ELISA using goat anti-rat IgG (Kirkegaard & Perry Laboratories), recombinant mouse IFNγ, biotinylated goat anti-mouse IFNγ and streptavidin-horseradish peroxidase (all from R&D Systems). Optical density (OD) was measured at 450 nm with a 570 nm reference filter.

For treatment experiments, XMG1.2 and Y13-259 antibodies were used. Intraperitoneal antibody treatment was performed with 0.5 mg antibody/mouse every 3rd day. A hybridoma producing XMG1.2 (a rat IgG1 monoclonal antibody directed against mouse IFNγ) (Cherwinski et al, 1987) was used for antibody production in mouse ascites. Affinity chromatography purification on protein G Sepharose was performed by BIOTEM (Le Rivier d'Apprieu, France). The control antibody Y13-259 (ATCC CRL-1742, a rat IgG1 antibody directed against RAS p21) was produced using a recombinant mammalian expression system.

Immunohistochemistry was performed using cell and tissue staining kits (R&D Systems) with monoclonal rat IgG2b anti-mouse macrophage antigen F4/80, monoclonal rat IgG1 anti-human CD3 crossreacting with mouse CD3 (clone CD3-12), rat IgG1 negative control (all from Serotec AbD), rat IgG2b negative control (Pharmingen), GRB7 (a monoclonal rabbit anti-granzyme B7) (Santa Cruz), rabbit serum (as a negative control) and biotinylated mouse IgG1 (as a negative control). The hybridoma producing KL-25 (a monoclonal mouse IgG1 anti-LCMV WE GP-1) was kindly provided by Professor Michael Buchmeier (Scripps Research Institute, USA) in agreement with Professor Demetrius Moskophidis (Medical College of Georgia, USA) (Bruns et al, 1983). KL-25 antibody (produced and purified by BIOTEM) was biotinylated using Biotin-X-NHS (Calbiochem). Immunohistochemistry was performed on cryosections with the exception of F4/80 and its negative control, which were used on paraffin-embedded sections, pretreated with Proteinase K (20 mg/ml, 3 min). Counterstaining was performed with haematoxylin. Images from immunohistochemistry experiments with negative control antibodies are not shown.

Organ weight and pathology

Organs were removed from sacrificed mice that had been infused with 20 ml of 4°C phosphate buffered saline (PBS) containing 2 mM EDTA. Total body weight was measured before infusion, while organ weight was measured after infusion and removal. Tissues were fixed in formalin 4% for 24 h, embedded in paraffin and stained with haematoxylin and eosin. Alternatively, tissues were fixed in 4% paraformaldehyde, cryoprotected by sucrose 30%, embedded in Cryomolds (Siemens Medical Solutions DIAG SAS) and snap frozen in liquid nitrogen. Light microscopy was performed using Axioplan 2 microscope (Zeiss), a QICAM Fast 1394 camera and Qcapture software (Qimaging).

Cells and cell culture

RAW264.7 cells (ATCC TIB-71) were cultured in RPMI 1640 medium with 2.05 mM L-glutamine (GIBCO) supplemented with 5% (v/v) heat-inactivated fetal bovine serum. Mouse sera were added directly to the culture medium (using the same dilution for all sera) and thereafter incubated with RAW264.7 cells at 37°C, 5% CO_2 for 4 h.

The paper explained

PROBLEM:

Haemophagocytic lymphohistiocytosis (HLH) is a potentially fatal inflammatory disease. It is characterized by fever, an enlarged spleen, cytopenia, elevated blood ferritin, coagulopathy, blood lipid changes and may also lead to neurological involvement. These symptoms are the result of hypercytokinaemia and organ infiltration by lymphocytes and macrophages. Current immunosuppressive and chemotherapeutic treatments needed to decrease inflammation can have serious side effects and there is a pressing need for effective, less toxic treatments in this disease.

RESULTS:

This manuscript shows that *in vivo* IFNγ neutralization has a dramatic curative effect on clinical and biological manifestations of experimental HLH. Therapeutic administration of an anti-IFNγ antibody to two different murine models of human hereditary HLH (perforin-deficient and Rab27a-deficient mice, both induced by lymphocytic choriomeningitis virus) ameliorated many of the HLH-related symptoms described above and induced recovery from the disease.

IMPACT:

This study proves the therapeutic efficacy of anti-IFNγ antibodies in experimental HLH and could be considered as a preclinical approach of an alternative HLH treatment.

Quantitative PCR

RNA was isolated from tissue samples and RAW264.7 cell cultures using the RNeasy Mini Kit (Qiagen), depleted in genomic DNA and then reverse transcribed into c-DNA using Quantitect (Qiagen).

LCMV: cDNA-preparations from five mouse livers (12–27 days after LCMV infection) were sequenced for LCMV to make sure that there were no mutations in the LCMV WE NP that would interfere with quantitative PCR analysis. In order to estimate the LCMV copy number, PCR products from β-actin and LCMV NP were cloned into pCR2.1-TOPO using *XhoI* forward primer: 5′-CTCGAGAAGGTGTGAT-3′, *NotI* reverse primer: 5′-TGCTTCTAGGCGGACTGCGGCC-3′ and *SacI* forward primer: 5′-GAGCTCGAGTCCTTCACATCCCAAAC-3′ and *SpeI* reverse primer: 5′-ACTAGTATCAAGGACGCAACCAGT-3′, respectively, and according to standard protocols (New England Biolabs). Quantitative PCR was performed on cDNA isolated from tissue samples and on the pCR2.1-TOPO plasmid containing β-actin and LCMV inserts using SYBR Green PCR Master mix (Applied Biosystems) and the following primers: LCMV: forward: 5′-TCTCATCCCAACCATTTGCA-3′ and reverse: 5′-GGGAAATTT-GACAGCACAACAA-3′; β-actin: forward: 5′-CCAGCAGATGTGGATCAGCA-3′ and reverse: 5′-CTTGCGGTGCACGATGG-3′.

IGTP: Quantitative PCR was performed on cDNA isolated from RAW264.7 cell culture samples using TaqMan Universal PCR Master mix (Applied Biosystems), a pre-designed gene expression assay for mouse IGTP and the following β-actin-probe: FAM-5′-CAGGAGTAC-GATGAGTCCGGCCCC-3′–TAMRA with the following primers for β-actin: forward: 5′-CCAGCAGATGTGGATCAGCA-3′ and reverse: 5′-CTTGCGGTGCACGATGG-3′.

Fluorescence measurement during PCR (and subsequent dissociation, if using SYBR Green) was performed on an ABI 7900 cycler and analysed using Sequence Detection Systems software (version 2.2.2, Applied Biosystems).

Statistical analysis

Analyses were performed with Prism version 4 for Macintosh (Graphpad). Survival curves were compared using the Logrank test. All other statistical hypotheses were analysed using *t*-tests.

Acknowledgements

The authors thank Professor Olivier Bernard, Professor Francis Jaubert, Professor Bernard Lacour, Marion Dupuis, Virginie Grondin, Michèle Malassis-Séris, Nathalie Prince, Catherine Schaffner, Dr Darin K. Fogg, Yoan Moreau, Nicolas Stadler and Dr Joey Ting for their assistance. This work was supported by grants from the Institut National de la Santé et de la Recherche Médicale (INSERM), the Agence Nationale de la Recherche (ANR-05-MIM-010 & BLAN06-3_145379), the Fondation pour la Recherche Médicale (Equipe labélisée FRM 2007) and through Coordination Theme 1 of the European Community's FP7, grant agreement number HEALTH-F2-2008-201461. JPS received grants from the Swiss Foundation for Grants in Medicine and Biology SSMBS (Swiss National Science Foundation) no. 1211/PASMA-110658/1, from the Fondazione Ettore e Valeria Rossi and the Walter und Gertrud Siegenthaler Stiftung.

Supporting information is available at EMBO Molecular Medicine online.

The authors have no financial or commercial conflicts of interest to declare.

For more information

OMIM, Online Mendelian Inheritance in Man:
FHL type 2:
http://www.ncbi.nlm.nih.gov/entrez/dispomim.cgi?id=603553
Perforin:
http://www.ncbi.nlm.nih.gov/entrez/dispomim.cgi?id=170280
Grisceli syndrome type 2:
http://www.ncbi.nlm.nih.gov/entrez/dispomim.cgi?id=607624
Rab27a:
http://www.ncbi.nlm.nih.gov/entrez/dispomim.cgi?id=603868

Histiocyte Society:
http://www.histiocytesociety.org

References

Abbott NJ, Ronnback L, Hansson E (2006) Astrocyte-endothelial interactions at the blood-brain barrier. Nat Rev Neurosci 7: 41-53

Badovinac VP, Hamilton SE, Harty JT (2003) Viral infection results in massive CD8+ T cell expansion and mortality in vaccinated perforin-deficient mice. Immunity 18: 463-474

Barbosa MD, Nguyen QA, Tchernev VT, Ashley JA, Detter JC, Blaydes SM, Brandt SJ, Chotai D, Hodgman C, Solari RC, Lovett M, Kingsmore SF (1996) Identification of the homologous beige and Chediak-Higashi syndrome genes. Nature 382: 262-265

Battegay M, Cooper S, Althage A, Banziger J, Hengartner H, Zinkernagel RM (1991) Quantification of lymphocytic choriomeningitis virus with an immunological focus assay in 24- or 96-well plates. J Virol Methods 33: 191-198

Billiau AD, Roskams T, Van Damme-Lombaerts R, Matthys P, Wouters C (2005) Macrophage activation syndrome: characteristic findings on liver biopsy illustrating the key role of activated, IFN-gamma-producing lymphocytes and IL-6- and TNF-alpha-producing macrophages. Blood 105: 1648-1651

Binder D, van den Broek MF, Kagi D, Bluethmann H, Fehr J, Hengartner H, Zinkernagel RM (1998) Aplastic anemia rescued by exhaustion of cytokine-secreting CD8+ T cells in persistent infection with lymphocytic choriomeningitis virus. J Exp Med 187: 1903-1920

Bruns M, Cihak J, Muller G, Lehmann-Grube F (1983) Lymphocytic choriomeningitis virus. VI. Isolation of a glycoprotein mediating neutralization. Virology 130: 247-251

Cherwinski HM, Schumacher JH, Brown KD, Mosmann TR (1987) Two types of mouse helper T cell clone. III. Further differences in lymphokine synthesis between Th1 and Th2 clones revealed by RNA hybridization, functionally monospecific bioassays, and monoclonal antibodies. J Exp Med 166: 1229-1244

Corne J, Djukanovic R, Thomas L, Warner J, Botta L, Grandordy B, Gygax D, Heusser C, Patalano F, Richardson W, Kilchherr E, Staehelin T, Davis F, Gordon W, Sun L, Liou R, Wang G, Chang TW, Holgate S (1997) The effect of intravenous administration of a chimeric anti-IgE antibody on serum IgE levels in atopic subjects: efficacy, safety, and pharmacokinetics. J Clin Invest 99: 879-887

Crozat K, Hoebe K, Ugolini S, Hong NA, Janssen E, Rutschmann S, Mudd S, Sovath S, Vivier E, Beutler B (2007) Jinx, an MCMV susceptibility phenotype caused by disruption of Unc13d: a mouse model of type 3 familial hemophagocytic lymphohistiocytosis. J Exp Med 204: 853-863

Czar MJ, Kersh EN, Mijares LA, Lanier G, Lewis J, Yap G, Chen A, Sher A, Duckett CS, Ahmed R, Schwartzberg PL (2001) Altered lymphocyte responses and cytokine production in mice deficient in the X-linked lymphoproliferative disease gene SH2D1A/DSHP/SAP. Proc Natl Acad Sci USA 98: 7449-7454

Emmenegger U, Schaer DJ, Larroche C, Neftel KA (2005) Haemophagocytic syndromes in adults: current concepts and challenges ahead. Swiss Med Wkly 135: 299-314

Feldmann J, Callebaut I, Raposo G, Certain S, Bacq D, Dumont C, Lambert N, Ouachee-Chardin M, Chedeville G, Tamary H, Minard-Colin V, Vilmer E, Blanche S, Le Deist F, Fischer A, de Saint Basile G (2003) Munc13-4 is essential for cytolytic granules fusion and is mutated in a form of familial hemophagocytic lymphohistiocytosis (FHL3). Cell 115: 461-473

Feldmann J, Le Deist F, Ouachee-Chardin M, Certain S, Alexander S, Quartier P, Haddad E, Wulffraat N, Casanova JL, Blanche S, Fischer A, de Saint Basile G (2002) Functional consequences of perforin gene mutations in 22 patients with familial haemophagocytic lymphohistiocytosis. Br J Haematol 117: 965-972

Fischer A, Cerf-Bensussan N, Blanche S, Le Deist F, Bremard-Oury C, Leverger G, Schaison G, Durandy A, Griscelli C (1986) Allogeneic bone marrow transplantation for erythrophagocytic lymphohistiocytosis. J Pediatr 108: 267-270

Gazit R, Aker M, Elboim M, Achdout H, Katz G, Wolf DG, Katzav S, Mandelboim O (2007) NK cytotoxicity mediated by CD16 but not by NKp30 is functional in Griscelli syndrome. Blood 109: 4306-4312

Henter JI, Arico M, Egeler RM, Elinder G, Favara BE, Filipovich AH, Gadner H, Imashuku S, Janka-Schaub G, Komp D, Ladisch S, Webb D (1997) HLH-94: a treatment protocol for hemophagocytic lymphohistiocytosis. HLH study Group of the Histiocyte Society. Med Pediatr Oncol 28: 342-347

Henter JI, Elinder G, Soder O, Hansson M, Andersson B, Andersson U (1991) Hypercytokinemia in familial hemophagocytic lymphohistiocytosis. Blood 78: 2918-2922

Henter JI, Horne A, Arico M, Egeler RM, Filipovich AH, Imashuku S, Ladisch S, McClain K, Webb D, Winiarski J, Janka G (2007) HLH-2004: Diagnostic and therapeutic guidelines for hemophagocytic lymphohistiocytosis. Pediatr Blood Cancer 48: 124-131

Hommes DW, Mikhajlova TL, Stoinov S, Stimac D, Vucelic B, Lonovics J, Zakuciova M, D'Haens G, Van Assche G, Ba S, Lee S, Pearce T (2006) Fontolizumab, a humanised anti-interferon gamma antibody, demonstrates safety and clinical activity in patients with moderate to severe Crohn's disease. Gut 55: 1131-1137

Horne A, Ramme KG, Rudd E, Zheng C, Wali Y, al-Lamki Z, Gurgey A, Yalman N, Nordenskjold M, Henter JI (2008) Characterization of PRF1, STX11 and UNC13D genotype-phenotype correlations in familial hemophagocytic lymphohistiocytosis. Br J Haematol 143: 75-83

Hsieh SM, Chang SC (2006) Insufficient perforin expression in CD8+ T cells in response to hemagglutinin from avian influenza (H5N1) virus. J Immunol 176: 4530-4533

Jordan MB, Filipovich AH (2008) Hematopoietic cell transplantation for hemophagocytic lymphohistiocytosis: a journey of a thousand miles begins with a single (big) step. Bone Marrow Transplant 42: 433-437

Jordan MB, Hildeman D, Kappler J, Marrack P (2004) An animal model of hemophagocytic lymphohistiocytosis (HLH): CD8+ T cells and interferon gamma are essential for the disorder. Blood 104: 735-743

Kunar V, Fausto N, Abbas A (2005) *Robbins and Cotran Pathologic Basis of Disease. St. Louis, MO,* Elsevier Inc.

Lainee P, Efron P, Tschoeke SK, Elies L, De Winter H, Lorre K, Moldawer LL (2005) Delayed neutralization of interferon-gamma prevents lethality in primate Gram-negative bacteremic shock. Crit Care Med 33: 797-805

Mahlaoui N, Ouachee-Chardin M, de Saint Basile G, Neven B, Picard C, Blanche S, Fischer A (2007) Immunotherapy of familial hemophagocytic lymphohistiocytosis with antithymocyte globulins: a single-center retrospective report of 38 patients. Pediatrics 120: 622-628

Mamishi S, Modarressi MH, Pourakbari B, Tamizifar B, Mahjoub F, Fahimzad A, Alyasin S, Bemanian MH, Hamidiyeh AA, Fazlollahi MR, Ashrafi MR, Isaeian A, Khotaei G, Yeganeh M, Parvaneh N (2008) Analysis of RAB27A gene in griscelli syndrome type 2: novel mutations including a deletion hotspot. J Clin Immunol 28: 384-389

Mansouri D, Adimi P, Mirsaeidi M, Mansouri N, Khalilzadeh S, Masjedi MR, Adimi P, Tabarsi P, Naderi M, Filipe-Santos O, Vogt G, de Beaucoudrey L, Bustamante J, Chapgier A, Feinberg J, Velayati AA, Casanova JL (2005) Inherited disorders of the IL-12-IFN-gamma axis in patients with disseminated BCG infection. Eur J Pediatr 164: 753-757

Mazodier K, Marin V, Novick D, Farnarier C, Robitail S, Schleinitz N, Veit V, Paul P, Rubinstein M, Dinarello CA, Harle JR, Kaplanski G (2005) Severe imbalance of IL-18/IL-18BP in patients with secondary hemophagocytic syndrome. Blood 106: 3483-3489

Menasche G, Pastural E, Feldmann J, Certain S, Ersoy F, Dupuis S, Wulffraat N, Bianchi D, Fischer A, Le Deist F, de Saint Basile G (2000) Mutations in RAB27A cause Griscelli syndrome associated with haemophagocytic syndrome. Nat Genet 25: 173-176

Metcalf D (2005) *Blood lines, an introduction to characterizing blood diseases of the post-genomic mouse. Durham, NC,* AlphaMed Press.

Moskophidis D, Battegay M, Bruendler MA, Laine E, Gresser I, Zinkernagel RM (1994) Resistance of lymphocytic choriomeningitis virus to alpha/beta interferon and to gamma interferon. J Virol 68: 1951-1955

Nagasawa M, Yi Z, Imashuku S, Nonoyama S, Ogawa K, Okumura K, Mizutani S (2008) Soluble TWEAK is markedly elevated in hemophagocytic lymphohistiocytosis. Am J Hematol 83: 222-225

Nagle DL, Karim MA, Woolf EA, Holmgren L, Bork P, Misumi DJ, McGrail SH, Dussault BJ Jr, Perou CM, Boissy RE, Duyk GM, Spritz RA, Moore KJ (1996) Identification and mutation analysis of the complete gene for Chediak-Higashi syndrome. Nat Genet 14: 307-311

Nansen A, Jensen T, Christensen JP, Andreasen SO, Ropke C, Marker O, Thomsen AR (1999) Compromised virus control and augmented perforin-mediated immunopathology in IFN-gamma-deficient mice infected with lymphocytic choriomeningitis virus. J Immunol 163: 6114-6122

Osugi Y, Hara J, Tagawa S, Takai K, Hosoi G, Matsuda Y, Ohta H, Fujisaki H, Kobayashi M, Sakata N, Kawa-Ha K, Okada S, Tawa A (1997) Cytokine production regulating Th1 and Th2 cytokines in hemophagocytic lymphohistiocytosis. Blood 89: 4100-4103

Pachlopnik Schmid J, Ho CH, Diana J, Pivert G, Lehuen A, Geissmann F, Fischer A, de Saint Basile G (2008) A Griscelli syndrome type 2 murine model of hemophagocytic lymphohistiocytosis (HLH). Eur J Immunol 38: 3219-3225

Perou CM, Moore KJ, Nagle DL, Misumi DJ, Woolf EA, McGrail SH, Holmgren L, Brody TH, Dussault BJ Jr, Monroe CA, Duyk GM, Pryor RJ, Li L, Justice MJ, Kaplan J (1996) Identification of the murine beige gene by YAC complementation and positional cloning. Nat Genet 13: 303-308

Plebani A, Ciravegna B, Ponte M, Mingari MC, Moretta L (2000) Interleukin-2 mediated restoration of natural killer cell function in a patient with Griscelli syndrome. Eur J Pediatr 159: 713-714

Polavarapu R, Gongora MC, Winkles JA, Yepes M (2005) Tumor necrosis factor-like weak inducer of apoptosis increases the permeability of the neurovascular unit through nuclear factor-kappa B pathway activation. J Neurosci 25: 10094-10100

Reinisch W, Hommes DW, Van Assche G, Colombel JF, Gendre JP, Oldenburg B, Teml A, Geboes K, Ding H, Zhang L, Tang M, Cheng M, van Deventer SJ, Rutgeerts P, Pearce T (2006) A dose escalating, placebo controlled, double blind, single dose and multidose, safety and tolerability study of fontolizumab, a humanised anti-interferon gamma antibody, in patients with moderate to severe Crohn's disease. Gut 55: 1138-1144

Rojas JR, Taylor RP, Cunningham MR, Rutkoski TJ, Vennarini J, Jang H, Graham MA, Geboes K, Rousselle SD, Wagner CL (2005) Formation, distribution, and elimination of infliximab and anti-infliximab immune complexes in cynomolgus monkeys. J Pharmacol Exp Ther 313: 578-585

Rottman M, Soudais C, Vogt G, Renia L, Emile JF, Decaluwe H, Gaillard JL, Casanova JL (2008) IFN-gamma mediates the rejection of haematopoietic stem cells in IFN-gammaR1-deficient hosts. PLoS Med 5: e26 (152-163)

Skurkovich S, Kasparov A, Narbut N, Skurkovich B (2002) Treatment of corneal transplant rejection in humans with anti-interferon-gamma antibodies. Am J Ophthalmol 133: 829-830

Skurkovich S, Skurkovich B (2005) Anticytokine therapy, especially anti-interferon-gamma, as a pathogenetic treatment in TH-1 autoimmune diseases. Ann N Y Acad Sci 1051: 684-700

Stepp SE, Dufourcq-Lagelouse R, Le Deist F, Bhawan S, Certain S, Mathew PA, Henter JI, Bennett M, Fischer A, de Saint Basile G, Kumar V (1999) Perforin gene defects in familial hemophagocytic lymphohistiocytosis. Science 286: 1957-1959

Takada H, Takahata Y, Nomura A, Ohga S, Mizuno Y, Hara T (2003) Increased serum levels of interferon-gamma-inducible protein 10 and monokine induced by gamma interferon in patients with haemophagocytic lymphohistiocytosis. Clin Exp Immunol 133: 448-453

zur Stadt U, Schmidt S, Kasper B, Beutel K, Diler AS, Henter JI, Kabisch H, Schneppenheim R, Nurnberg P, Janka G, Hennies HC (2005) Linkage of familial hemophagocytic lymphohistiocytosis (FHL) type-4 to chromosome 6q24 and identification of mutations in syntaxin 11. Hum Mol Genet 14: 827-834

